SANDIA REPORT
SAND2015-9566
Unlimited Release
Printed October 2015

Phase Centers of Subapertures in a Tapered Aperture Array

Armin W. Doerry and Douglas L. Bickel

Prepared by
Sandia National Laboratories
Albuquerque, New Mexico 87185 and Livermore, California 94550

Sandia National Laboratories is a multi-program laboratory managed and operated by Sandia Corporation, a wholly owned subsidiary of Lockheed Martin Corporation, for the U.S. Department of Energy's National Nuclear Security Administration under contract DE-AC04-94AL85000.

Issued by Sandia National Laboratories, operated for the United States Department of Energy by Sandia Corporation.

Available to DOE and DOE contractors from

U.S. Department of Energy
Office of Scientific and Technical Information
P.O. Box 62
Oak Ridge, TN 37831

Telephone: (865) 576-8401
Facsimile: (865) 576-5728
E-Mail: reports@adonis.osti.gov
Online ordering: http://www.osti.gov/bridge

Available to the public from

U.S. Department of Commerce
National Technical Information Service
5285 Port Royal Rd.
Springfield, VA 22161

Telephone: (800) 553-6847
Facsimile: (703) 605-6900
E-Mail: orders@ntis.fedworld.gov
Online order: http://www.ntis.gov/help/ordermethods.asp?loc=7-4-0#online

SAND2015-9566
Unlimited Release
Printed October 2015

Phase Centers of Subapertures in a Tapered Aperture Array

Armin W. Doerry
ISR Mission Engineering

Douglas L. Bickel
ISR Analysis & Applications

Sandia National Laboratories
PO Box 5800
Albuquerque, NM 87185-0519

Abstract

Antenna apertures that are tapered for sidelobe control can also be parsed into subapertures for Direction of Arrival (DOA) measurements. However, the aperture tapering complicates phase center location for the subapertures, knowledge of which is critical for proper DOA calculation. In addition, tapering affects subaperture gains, making gain dependent on subaperture position. Techniques are presented to calculate subaperture phase center locations, and algorithms are given for equalizing subapertures' gains. Sidelobe characteristics and mitigation are also discussed.

Acknowledgements

This work was the result of an unfunded research and development activity.

Contents

Foreword

This report details the results of an academic study. It does not presently exemplify any modes, methodologies, or techniques employed by any operational system known to the authors.

Classification

The specific mathematics and algorithms presented herein do not bear any release restrictions or distribution limitations.

This distribution limitations of this report are in accordance with the classification guidance detailed in the memorandum “Classification Guidance Recommendations for Sandia Radar Testbed Research and Development”, DRAFT memorandum from Brett Remund (Deputy Director, RF Remote Sensing Systems, Electronic Systems Center) to Randy Bell (US Department of Energy, NA-22), February 23, 2004. Sandia has adopted this guidance where otherwise none has been given.

This report formalizes preexisting informal notes and other documentation on the subject matter herein.

1 Introduction & Background

The ability of a radar system to make Direction-of-Arrival (DOA) measurements, especially of moving targets, requires the ability to generate multiple antenna beams and compare responses from the collection. Techniques for this are well established in the literature. When more than two receive antenna beams are required along any one axis, the typical antenna architecture is to use distinct antenna subapertures with separated phase centers in a phase-monopulse configuration. We note that the IEEE Standard on Radar Definitions[1] describes monopulse as "A radar technique in which information concerning the angular location of a target is obtained by comparison of signals received in two *or more* [emphasis added] simultaneously antenna beams."

We also generally desire low sidelobe responses from the antenna, including its main reference beam, and to some extent even any other beams the antenna may generate in order to make its DOA calculations. Low sidelobe response generally requires beam shaping via antenna aperture tapering.

We will assume herein that we are dealing with a monostatic antenna configuration, wherein the same overall aperture is used for transmit and receive signals. We assume that the transmit signal will use the entire aperture, but the receive signal is collected by subapertures, wherein the subapertures are parsed from the larger overall sum aperture. That is, the sum of the individual receive subapertures equals the transmit aperture. This architecture complicates the nature of the receive subapertures in that they inherently have different characteristics, perhaps in beamwidth, gain, or both.

Nevertheless, of ultimate interest to the subsequent signal processing are the locations of the phase centers of the various subapertures, and the gains imparted to the subapertures' received signals. Knowledge of these is required for optimal DOA calculations.

We offer as background for this report several other previously published reports.

> SAND2013-10635 describes calculating a phase center for a dish reflector antenna.[2]
>
> SAND2015-2310 making DOA measurements from multi-subaperture antennas with uniform weighting.[3]
>
> SAND2015-2311 describes the limits of null widths in multi-subaperture antennas.[4]
>
> SAND2015-4113 describes designing a 3-beam amplitude monopulse antenna.[5]

Subsequently, herein we discuss locating the phase centers of uneven aperture illuminations, and of subapertures in overall tapered apertures. We confine our discussion to one-dimensional analysis and examples. We furthermore ignore many aspects of practical antenna design such as mutual coupling in array antennas, etc.

"The scientists of today think deeply instead of clearly. One must be sane to think clearly, but one can think deeply and be quite insane."
-- Nikola Tesla

2 Phase Center of Arbitrary Aperture Illumination

We begin by considering a linear aperture with illumination

$$w(z) = \text{normalized (domain) aperture illumination function,} \tag{1}$$

where the illumination function is limited to a finite extent such that

$$\int_{-\infty}^{x} w(z)\,dz = \int_{-\infty}^{x} w(z)\,\text{rect}(z)dz, \tag{2}$$

where

$$\text{rect}(z) = \begin{cases} 1 & |z| < 1/2 \\ 1/2 & |z| = 1/2 \\ 0 & else \end{cases}. \tag{3}$$

We define the rect( ) function this way to make later mathematics in this report more precise.

We now define a point on the linear axis, specified as the *x* axis, about which we rotate the aperture as

$$x_0 = \text{rotation point of the aperture.} \tag{4}$$

We furthermore define

$$\begin{aligned} x_1 &= \text{physical center the aperture, and} \\ L &= \text{actual length of the aperture,} \end{aligned} \tag{5}$$

This geometry is identified in Figure 1. The far-field pattern can then be calculated as

$$G(\theta) = \int_{x_1-L/2}^{x_1+L/2} w\left(\frac{x-x_1}{L}\right) e^{-j\frac{2\pi\sin\theta}{\lambda}(x-x_0)}\,dx, \tag{6}$$

where

$$\begin{aligned} \theta &= \text{Direction of Arrival (DOA) incidence angle, and} \\ \lambda &= \text{wavelength of the sinusoidal signal.} \end{aligned} \tag{7}$$

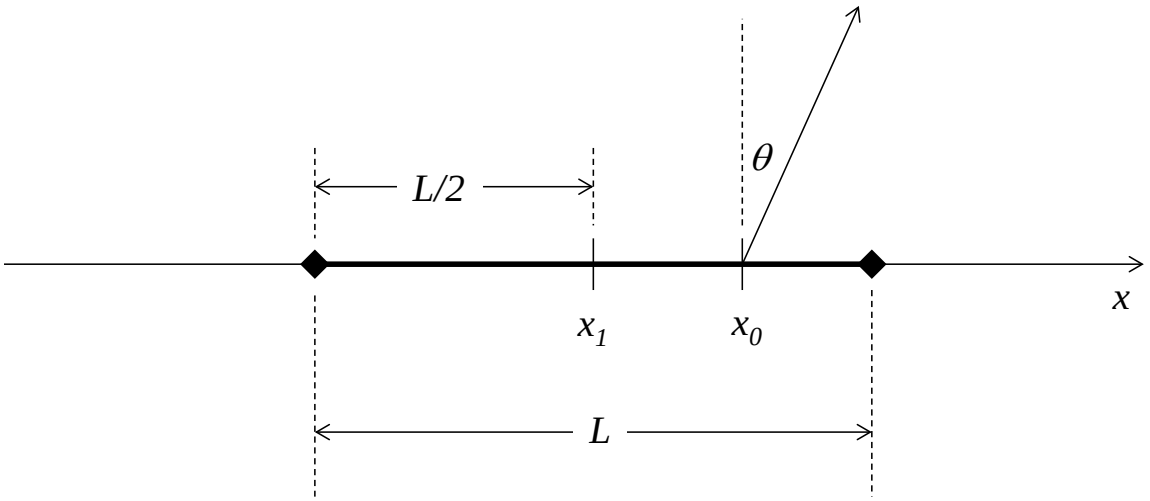

Figure 1. One-dimensional aperture geometry definitions. The aperture illumination is essentially the current distribution within the finite aperture.

Note that this is just the well-known axiom that the far-field antenna pattern is essentially a Fourier transform of the aperture illumination function.

In general, $G(\theta)$ is complex-valued. Our concern here is with a phase change in $G(\theta)$ as we vary θ. We desire the value of x_0 for which there is no phase change in $G(\theta)$ as θ is varied. The value of x_0 that accomplishes this is the "phase center" of the aperture.

We now examine two example cases.

2.1 Uniform Aperture Illumination

Consider the case where we have a uniformly illuminated aperture described by

$$w(z) = \text{rect}(z). \tag{8}$$

In this case, then the far-field pattern is given by

$$G(\theta) = \int_{x_1 - L/2}^{x_1 + L/2} e^{-j\frac{2\pi \sin\theta}{\lambda}(x - x_0)} dx, \tag{9}$$

where

$$\theta = \text{Direction of Arrival (DOA) incidence angle,} \tag{10}$$

which can be solved and simplified to

$$G(\theta) = e^{-j\frac{2\pi \sin\theta}{\lambda}(x_1 - x_0)} L \,\mathrm{sinc}\left(\frac{L}{\lambda}\sin\theta\right), \tag{11}$$

where

$$\mathrm{sinc}(z) = \frac{\sin(\pi z)}{\pi z}. \tag{12}$$

We identify the phase term as the exponent of the exponential factor, which shows a dependence on angle θ whenever $x_0 \neq x_1$. Consequently, the far-field pattern phase is independent of rotation angle θ when $x_0 = x_1$. Therefore, we identify the phase center for this aperture as

$$x_{pc} = x_1. \tag{13}$$

The aperture illumination and the phase center location for this example are illustrated in Figure 2, where we have arbitrarily presumed $x_1 = 0$.

We may furthermore stipulate that Fourier properties suggest that any even-symmetric and real $w(z)$ will result in $x_{pc} = x_1$.

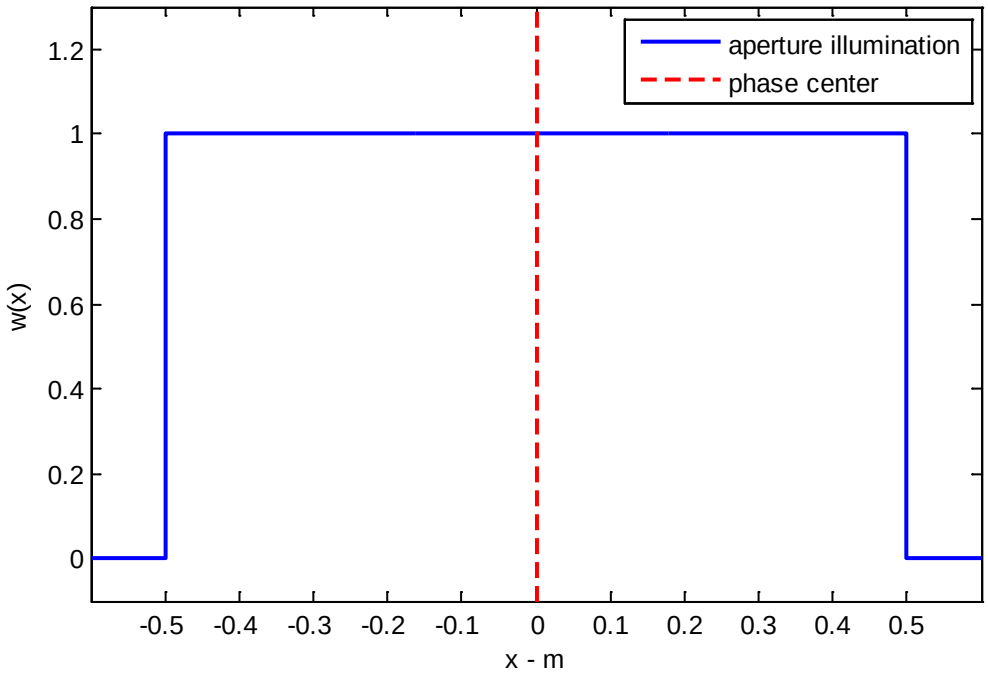

Figure 2. Uniform aperture illumination.

2.2 Linear-Gradient Aperture Illumination

Now consider an aperture illumination of the form

$$w(z) = (1+\alpha z)\,\mathrm{rect}(z) \tag{14}$$

where

$$\alpha \text{ = constant such that } 0 < \alpha < 1. \tag{15}$$

Note that this is not an even function, and definitely not uniform. In this case, the far-field pattern is then given by

$$G(\theta) = \int_{x_1 - L/2}^{x_1 + L/2} \left(1 + \alpha\left(\frac{x - x_1}{L}\right)\right) e^{-j\frac{2\pi \sin\theta}{\lambda}(x - x_0)}\, dx. \tag{16}$$

With no loss of generality, we will assume that $x_1 = 0$. We will then rewrite the far-field pattern as

$$G(\theta) = e^{j\frac{2\pi \sin\theta}{\lambda}x_0} \int_{-L/2}^{L/2} \left(1 + \frac{\alpha}{L}x\right) e^{-j\frac{2\pi \sin\theta}{\lambda}x}\, dx. \tag{17}$$

This can be solved to yield

$$G(\theta) = e^{j\frac{2\pi \sin\theta}{\lambda}x_0} \left\{ \begin{array}{l} L\,\mathrm{sinc}\left(\frac{L}{\lambda}\sin\theta\right) \\ -j\left(\frac{\alpha L}{2}\right)\left(\frac{\sin\left(\pi\frac{L}{\lambda}\sin\theta\right)}{\left(\pi\frac{L}{\lambda}\sin\theta\right)^2} - \frac{\cos\left(\pi\frac{L}{\lambda}\sin\theta\right)}{\left(\pi\frac{L}{\lambda}\sin\theta\right)} \right) \end{array} \right\}. \tag{18}$$

Recall that we desire to identify a phase center that is a single constant value for x_0 that results in a phase that is independent of angle θ. We may solve for the phase as

$$\mathrm{Phase}\left(G(\theta)\right) = \mathrm{atan}\left\{ \left(\frac{\alpha}{2}\right)\left(\cot\left(\pi\frac{L}{\lambda}\sin\theta\right) - \frac{1}{\left(\pi\frac{L}{\lambda}\sin\theta\right)} \right) \right\} + \frac{2\pi \sin\theta}{\lambda}x_0. \tag{19}$$

We can solve for a position x_0 that causes the phase to go to zero, and designate this as the phase center of the aperture. Doing so yields the phase center location as

$$x_{pc} = \frac{-\lambda}{2\pi \sin\theta} \operatorname{atan}\left\{ \left(\frac{\alpha}{2}\right) \left\{ \cot\left(\pi \frac{L}{\lambda} \sin\theta\right) - \frac{1}{\left(\pi \frac{L}{\lambda} \sin\theta\right)} \right\} \right\}. \tag{20}$$

We note that phase center x_{pc} is not a constant, and in fact actually depends on DOA angle θ. No single value of x_{pc} causes the phase to go to zero for all angles θ. That is, the phase center moves as a function of DOA angle θ. In the neighborhood of the center of the beam where $\theta \approx 0$ we may nevertheless choose a constant x_{pc} that minimizes dependence of $G(\theta)$ on angle θ by setting the derivative of Eq. (19) to zero and solving for the x_0 that causes a nearly constant phase in the neighborhood of $\theta = 0$. We identify the derivative of the phase in the direction of $\theta = 0$ as

$$\lim_{\theta \to 0} \left(\frac{d}{d\theta} \text{Phase}\left(G(\theta)\right) \right) = -\frac{\pi}{6\lambda} \left(\alpha L - 12 x_0\right). \tag{21}$$

Consequently, we designate the phase center as the value of x_0 that causes this to go to zero, namely

$$x_{pc} = \frac{L\alpha}{12}. \tag{22}$$

Essentially, the phase slope of $G(\theta)$ as a function of θ is zero with this value for x_0 at the angle $\theta = 0$.

We observe that the non-uniform aperture illumination in Figure 3 has the phase center indicated, as calculated above. Note that it is off-center with respect to the aperture center at $x_1 = 0$. Furthermore, it is shifted in the direction of heavier weighting of the aperture, as we might expect.

The far-field antenna pattern is illustrated in Figure 4, and the received signal phase as a function of rotation position and incidence DOA angle is shown in Figure 5. Note that rotating about the nominal phase center exhibits a fairly constant phase value within the mainlobe of the far-field pattern.

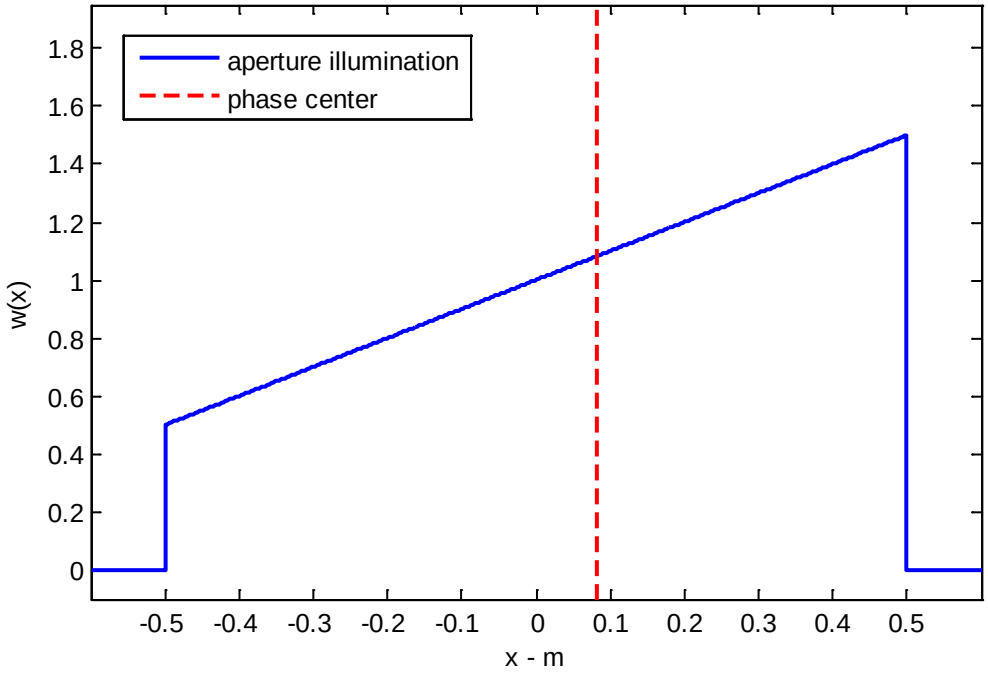

Figure 3. Example non-uniform aperture illumination.

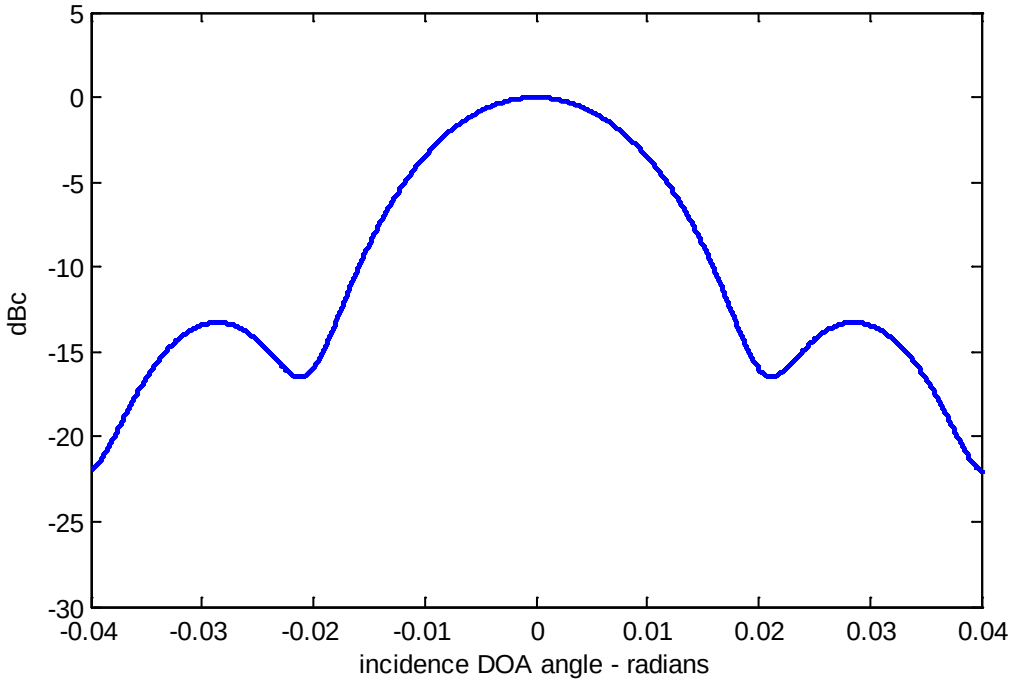

Figure 4. Far-field antenna pattern for illumination of Figure 3.

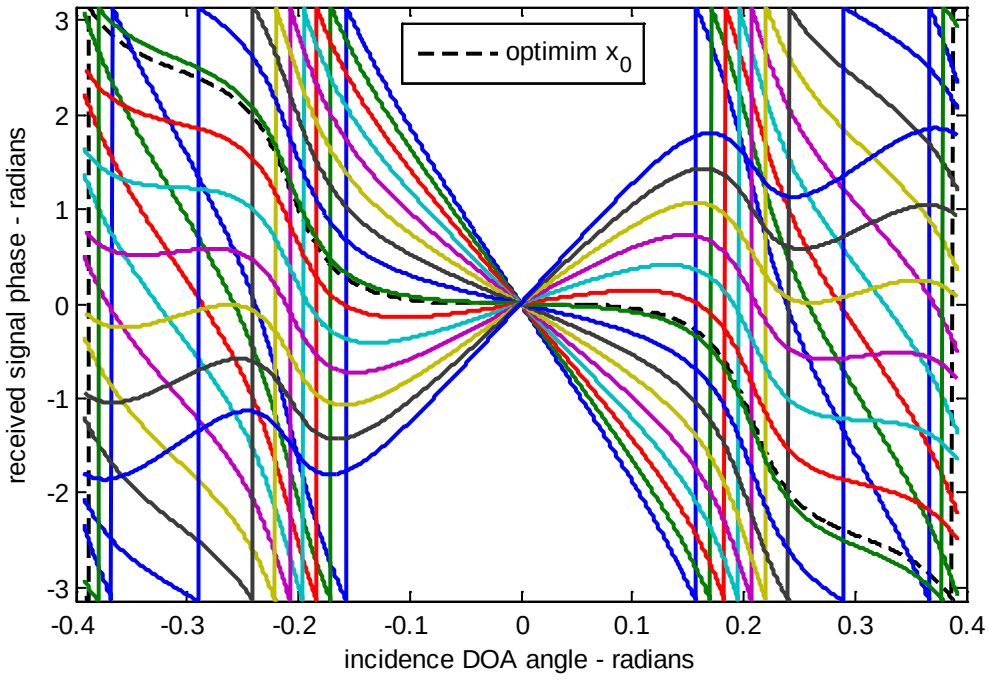

Figure 5. Received signal phase versus incidence DOA angle for various rotation positions x_0. The optimum x_0, that which is most flat at a zero DOA angle, indicates the phase center.

2.3 Comments

We offer the following additional comments.

- More complicated aperture illumination functions might cause us to use numerical techniques to estimate the phase center location.
- More complicated aperture illumination functions will generally have phase centers that are DOA angle dependent. However, some locations are more well-behaved than others, in minimizing phase variations over DOA angles of interest.
- Phase centers will be pulled in the direction of more weighting in the aperture.

“The value of an idea lies in the using of it.”
-- Thomas A. Edison

3 Subapertures in a Tapered Sum Pattern

We now build upon the previous section and examine a larger aperture composed of contiguous but non-overlapping subapertures, wherein the larger aperture has a specified taper function for sidelobe control of the overall combined, or sum, antenna beam.

We now modify and add the following definitions.

L_{ap} = physical length of the overall aperture,

$w_{ap}(x)$ = illumination (taper) function of the overall aperture,

i = index of phase centers, $i \in \{0,1,2,...,(I-1)\}$,

I = number of subapertures,

$x_{1,i}$ = physical center of the i^{th} subaperture,

$x_{pc,i}$ = phase center of the i^{th} subaperture,

L_i = physical length of the i^{th} subaperture. (23)

We will assume that $w_{ap}(x)$ is real and even, and nonzero over the interval $[-0.5, 0.5]$. Without loss of generality, we will also assume that the overall aperture is physically centered at zero.

The contiguous but non-overlapped nature of the subapertures is then such that

$$\text{rect}\left(\frac{x}{L_{ap}}\right) = \sum_{i=0}^{I-1} \text{rect}\left(\frac{x - x_{1,i}}{L_i}\right). \tag{24}$$

This basically means that they don't overlap, and there are no gaps. The far-field pattern for the overall aperture, also referred to as the "sum" beam, is calculated as

$$G_{ap}(\theta) = \int_{-\infty}^{\infty} w_{ap}\left(\frac{x}{L_{ap}}\right) e^{-j\frac{2\pi \sin\theta}{\lambda}x} dx, \tag{25}$$

whereas the far-field patterns of the individual subapertures are calculated as

$$G_i(\theta) = \int_{-\infty}^{\infty} \left[\text{rect}\left(\frac{x - x_{1,i}}{L_i}\right) w_{ap}\left(\frac{x}{L_{ap}}\right)\right] e^{-j\frac{2\pi \sin\theta}{\lambda}x} dx. \tag{26}$$

Note that the quantity in the square brackets represents the taper function of the individual subapertures. These individual subaperture tapers are real but not by themselves even.

Interestingly, a consequence of this is that the sum of the individual subaperture beams equals the overall sum pattern beam shape. That is

$$\sum_{i=0}^{I-1} G_i(\theta) = G_{ap}(\theta). \tag{27}$$

Recall that we have not yet specified the lengths of the individual subapertures; merely that they add up to the overall aperture length. Now we examine several specific cases.

3.1 Uniform Width Subapertures

We now assume that all subapertures have equal physical length. That is

$$L_i = L_k \text{, for all subaperture indices } i,k \ . \tag{28}$$

We illustrate with several examples.

For all subsequent examples, unless otherwise indicated, we shall assume an overall aperture weighting defined by a Taylor window with −30 dB sidelobes and $\bar{n} = 5$. Furthermore, we shall assume

$$\begin{aligned} L_{ap} &= 1 \text{ m, and} \\ \lambda &= 0.02 \text{ m.} \end{aligned} \tag{29}$$

Subaperture phase centers are calculated using numerical integration.

3.1.1 Three Subapertures

We illustrate with an example that divides the aperture into three equal-length subapertures. Relevant measures are given in Table 1. Figure 6 plots the subapertures and their phase centers. Figure 7 plots the one-way patterns. Figure 8 illustrates the two-way pattern, with the transmitted signal using the sum pattern. We observe that for this example there is nearly a 6 dB gain difference between center and outer subapertures.

Table 1. Subaperture characteristics for 3 subapertures using -30 dB Taylor window, $\bar{n} = 5$.

Subaperture	*Physical Center (m)*	*Phase Center (m)*	*Width (m)*	*Gain (dBc)*
0	–0.3333	–0.2966	0.3333	–11.8548
1	0	0	0.3333	–6.2111
2	0.3333	0.2966	0.3333	–11.8548

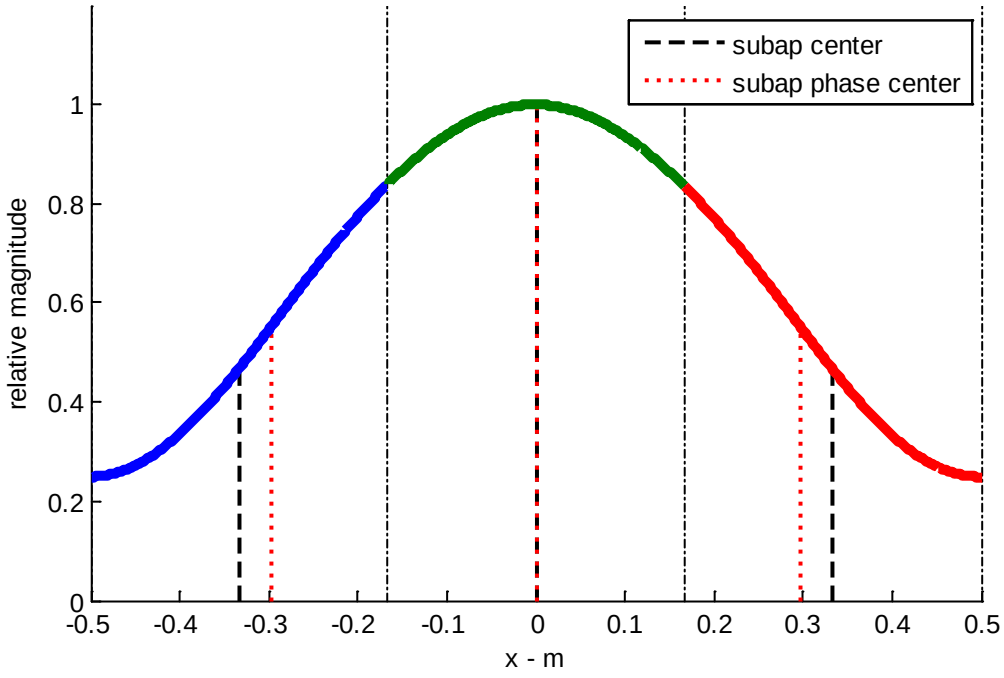

Figure 6. Subaperture definitions and parameters. Overall aperture weighting is –30 dB Taylor window with nbar=5.

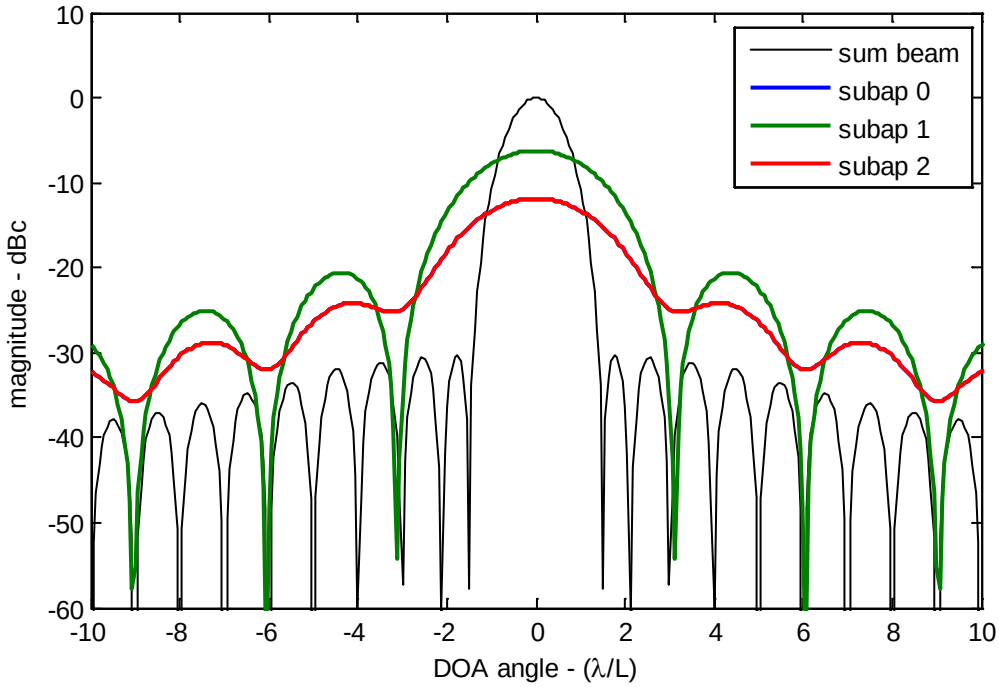

Figure 7. One-way beam patterns for overall aperture and subapertures.

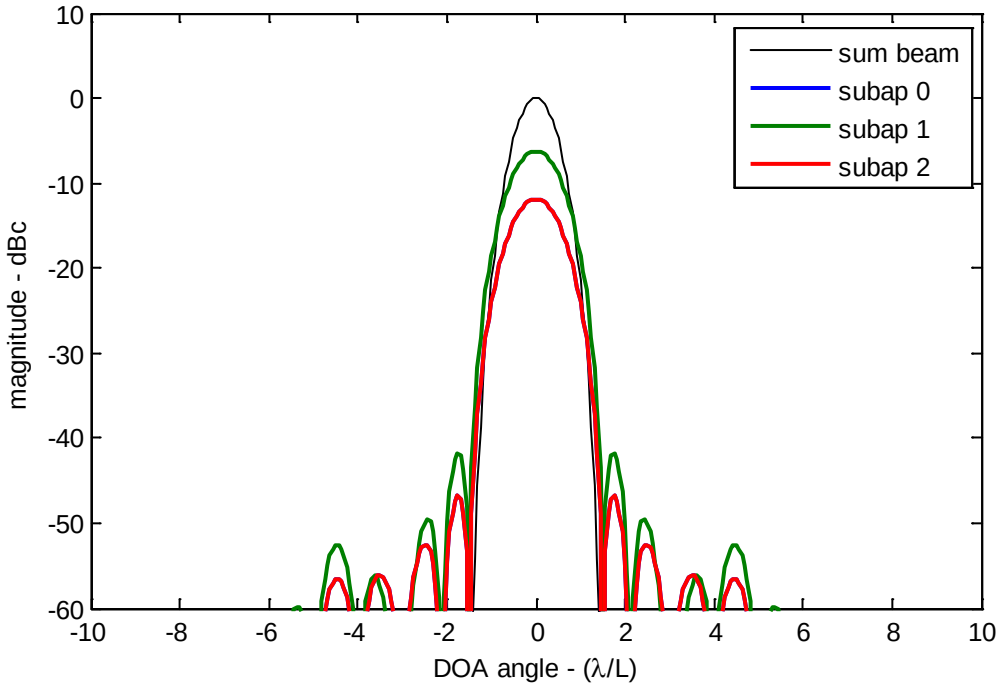

Figure 8. Two-way beam patterns for overall aperture and subapertures.

3.1.2 Four Subapertures

We illustrate with an example that divides the aperture into 4 equal-length subapertures. Relevant measures are given in Table 2. Figure 9 plots the subapertures and their phase centers. Figure 10 plots the one-way patterns. Figure 11 illustrates the two-way pattern, with the transmitted signal using the sum pattern. We observe that for this example there is nearly a 7 dB gain difference between center and outer subapertures.

Table 2. Subaperture characteristics for 4 subapertures using -30 dB Taylor window, $\bar{n} = 5$.

Subaperture	*Physical Center (m)*	*Phase Center (m)*	*Width (m)*	*Gain (dBc)*
0	–0.375	–0.3524	0.25	–16.0446
1	–0.125	–0.1168	0.25	–9.3113
2	0.125	0.1168	0.25	–9.3113
3	0.375	0.3524	0.25	–16.0446

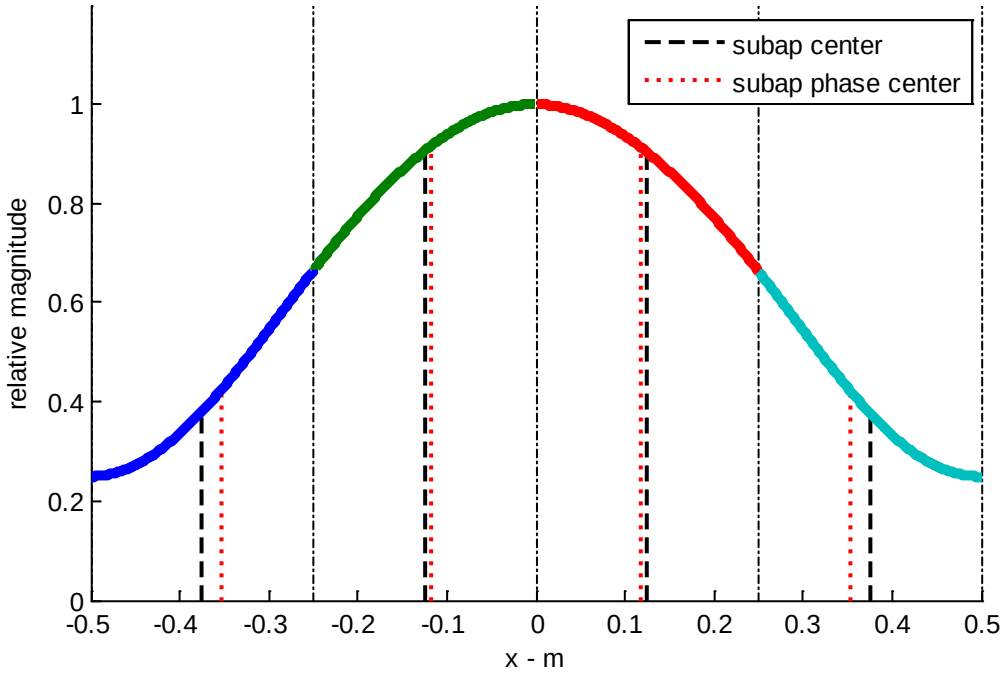

Figure 9. Subaperture definitions and parameters. Overall aperture weighting is –30 dB Taylor window with nbar=5.

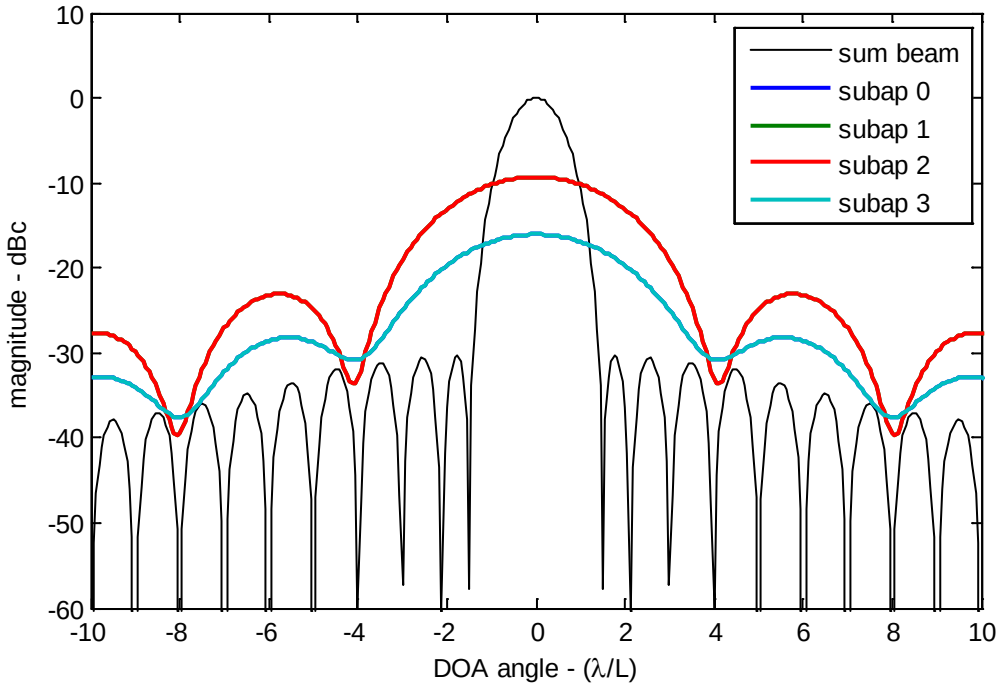

Figure 10. One-way beam patterns for overall aperture and subapertures.

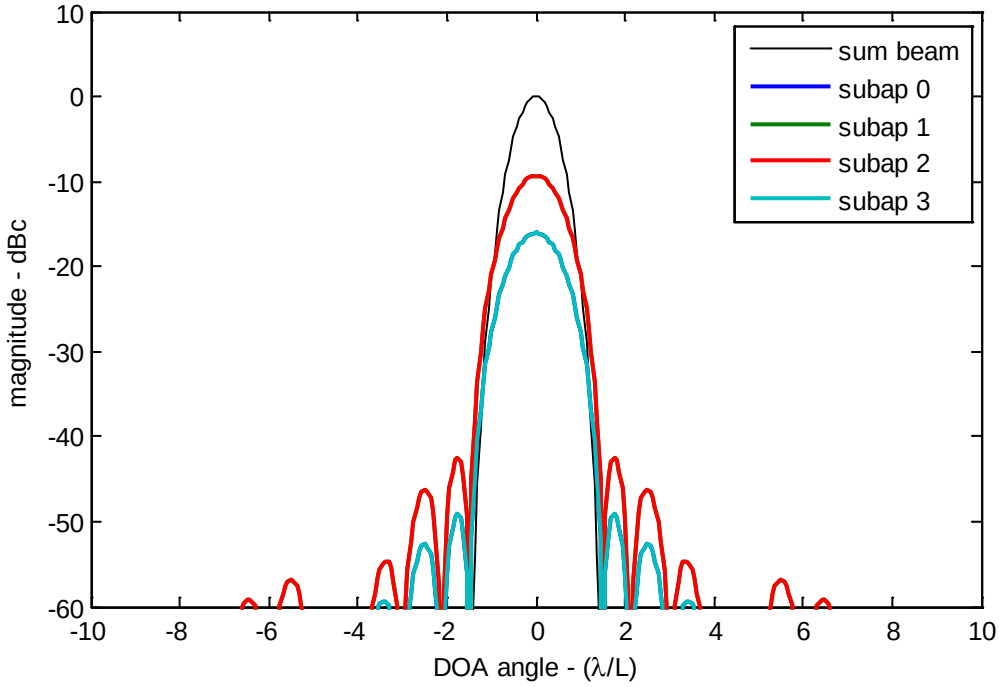

Figure 11. Two-way beam patterns for overall aperture and subapertures.

3.1.3 Five Subapertures

We illustrate with an example that divides the aperture into 5 equal-length subapertures. Relevant measures are given in Table 3. Figure 12 plots the subapertures and their phase centers. Figure 13 plots the one-way patterns. Figure 14 illustrates the two-way pattern, with the transmitted signal using the sum pattern. We observe that for this example there is nearly a 9 dB gain difference between center and outer subapertures.

Table 3. Subaperture characteristics for 5 subapertures using -30 dB Taylor window, $\bar{n} = 5$.

Subaperture	*Physical Center (m)*	*Phase Center (m)*	*Width (m)*	*Gain (dBc)*
0	–0.4	–0.3856	0.2	–19.1214
1	–0.2	–0.1913	0.2	–12.5004
2	0	0	0.2	–10.3295
3	0.2	0.1913	0.2	–12.5004
4	0.4	0.3856	0.2	–19.1214

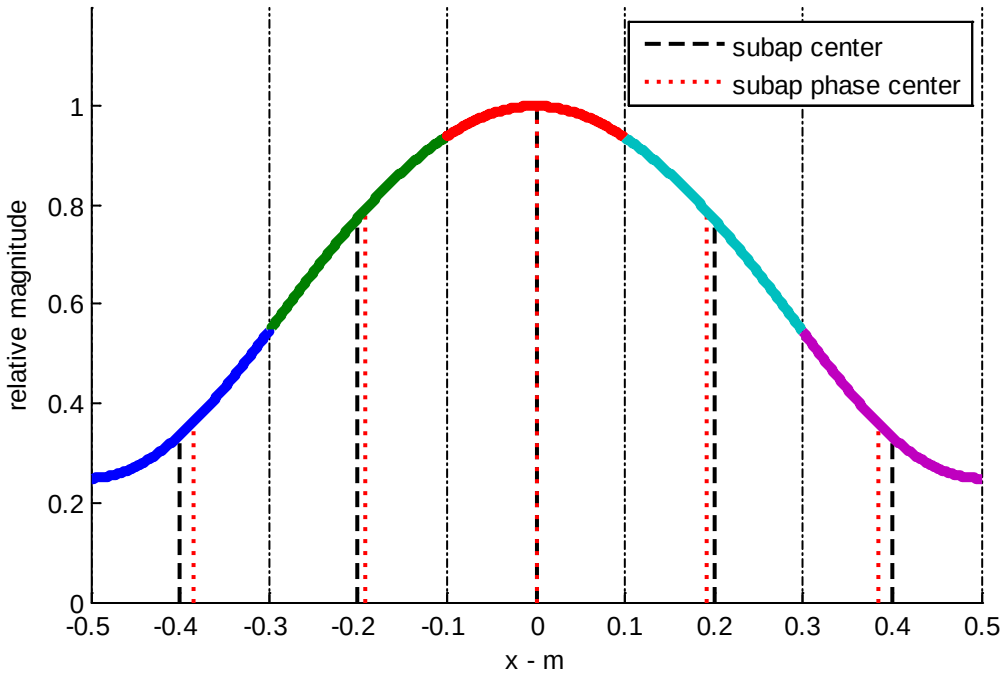

Figure 12. Subaperture definitions and parameters. Overall aperture weighting is –30 dB Taylor window with nbar=5.

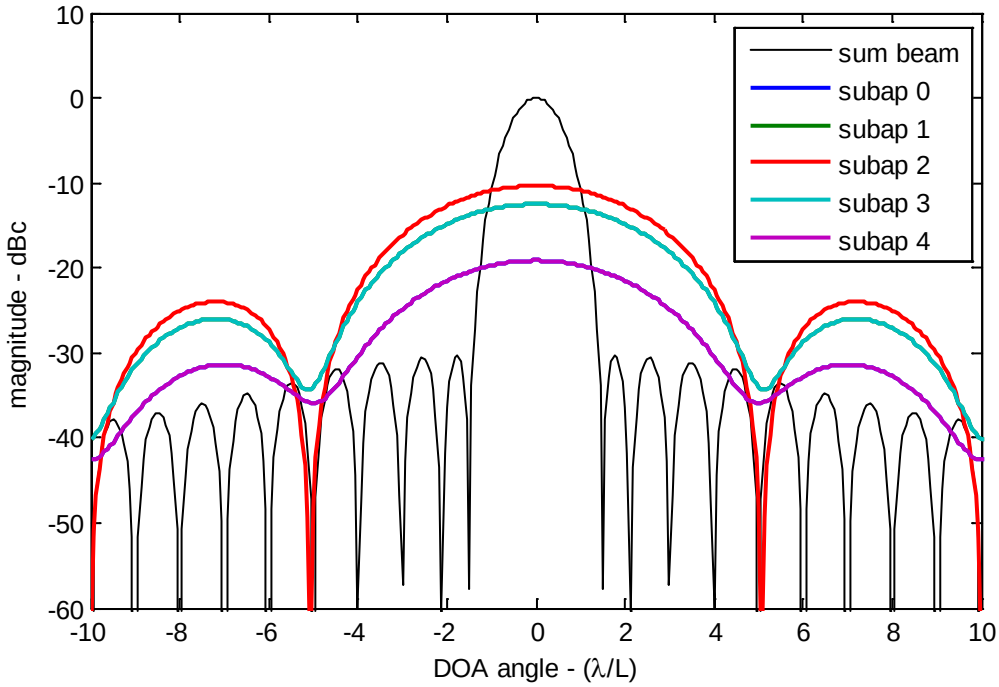

Figure 13. One-way beam patterns for overall aperture and subapertures.

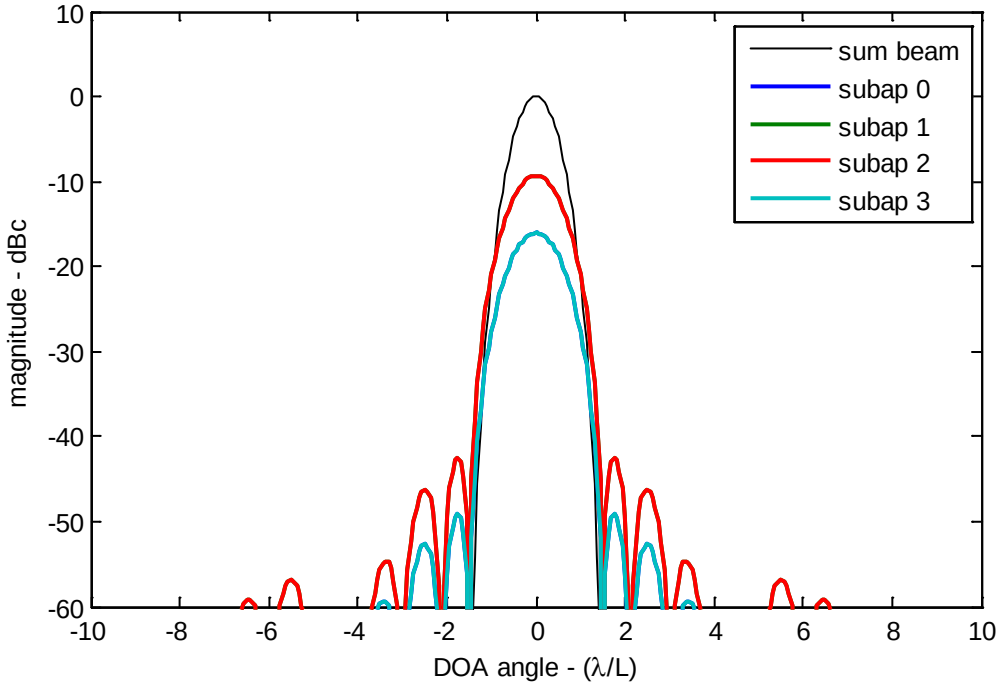

Figure 14. Two-way beam patterns for overall aperture and subapertures.

3.2 Uniform Gain Subapertures

We now assume that all subapertures have equal gain at the center of their patterns. That is

$$G_i(0) = G_k(0), \text{ for all subaperture indices } i,k \ . \tag{30}$$

To accomplish this, we will give up the constraint of equal widths.

We illustrate with several examples.

For all subsequent examples, unless otherwise indicated, we shall assume an overall aperture weighting defined by a Taylor window with −30 dB sidelobes and $\bar{n} = 5$. Furthermore, we shall assume

$$\begin{aligned} L_{ap} &= 1 \text{ m, and} \\ \lambda &= 0.02 \text{ m.} \end{aligned} \tag{31}$$

Subaperture phase centers are calculated using numerical integration.

3.2.1 Three Subapertures

We illustrate with an example that divides the aperture into three equal-gain subapertures. Relevant measures are given in Table 4. Figure 15 plots the subapertures and their phase centers. Figure 16 plots the one-way patterns. Figure 17 illustrates the two-way pattern, with the transmitted signal using the sum pattern.

Table 4. Subaperture characteristics for 3 subapertures using -30 dB Taylor window, $\bar{n} = 5$.

Subaperture	*Physical Center (m)*	*Phase Center (m)*	*Width (m)*	*Gain (dBc)*
0	–0.3050	–0.2595	0.39	–9.5425
1	0	0	0.2199	–9.5425
2	0.3050	0.2595	0.39	–9.5425

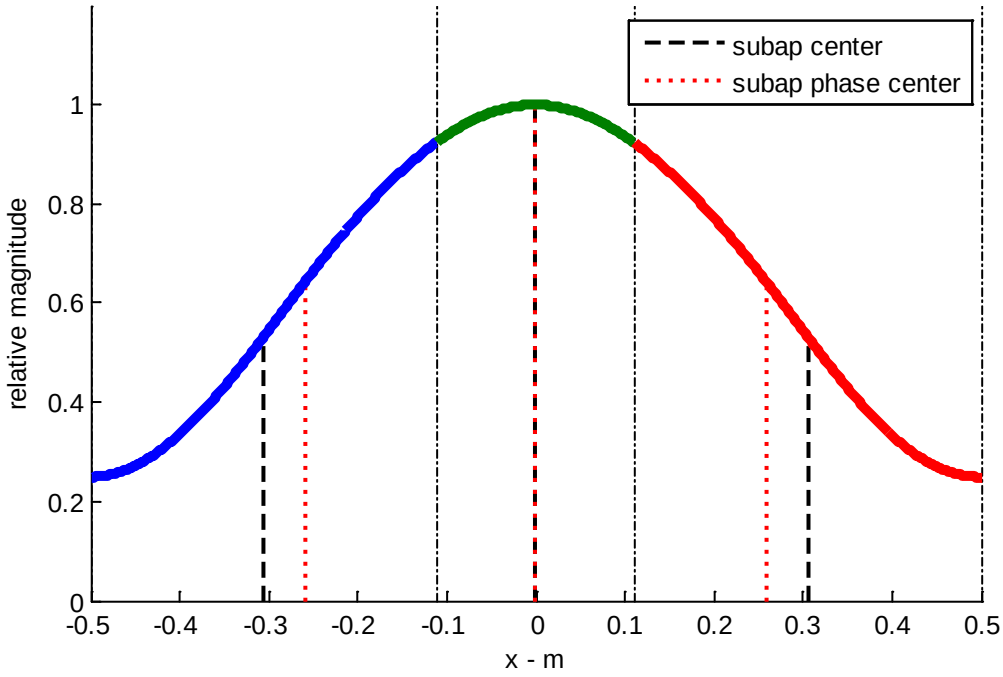

Figure 15. Subaperture definitions and parameters. Overall aperture weighting is –30 dB Taylor window with nbar=5.

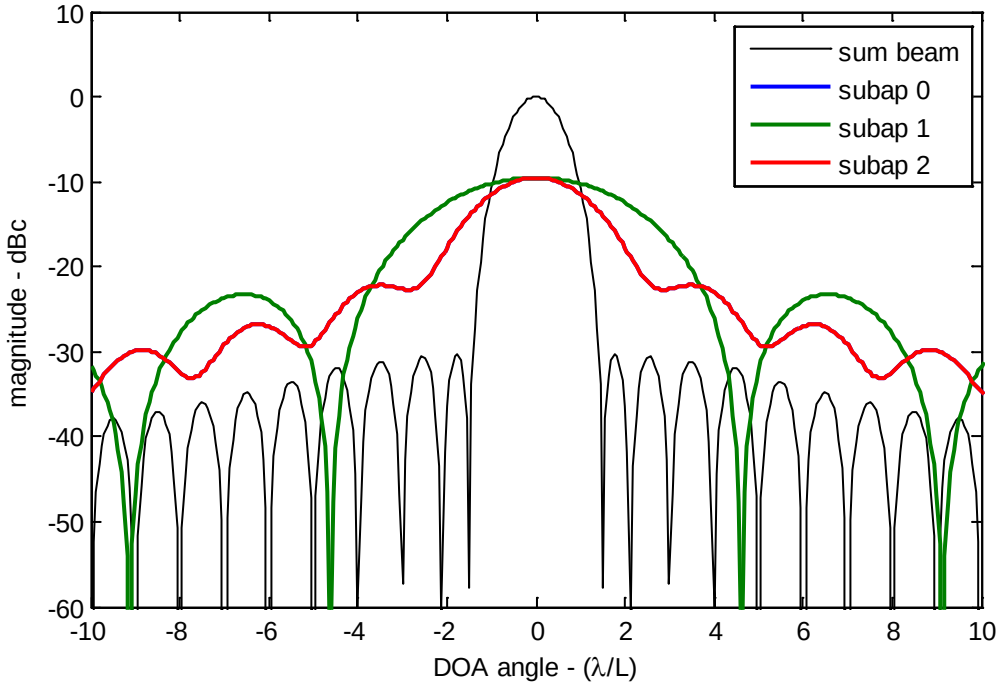

Figure 16. One-way beam patterns for overall aperture and subapertures.

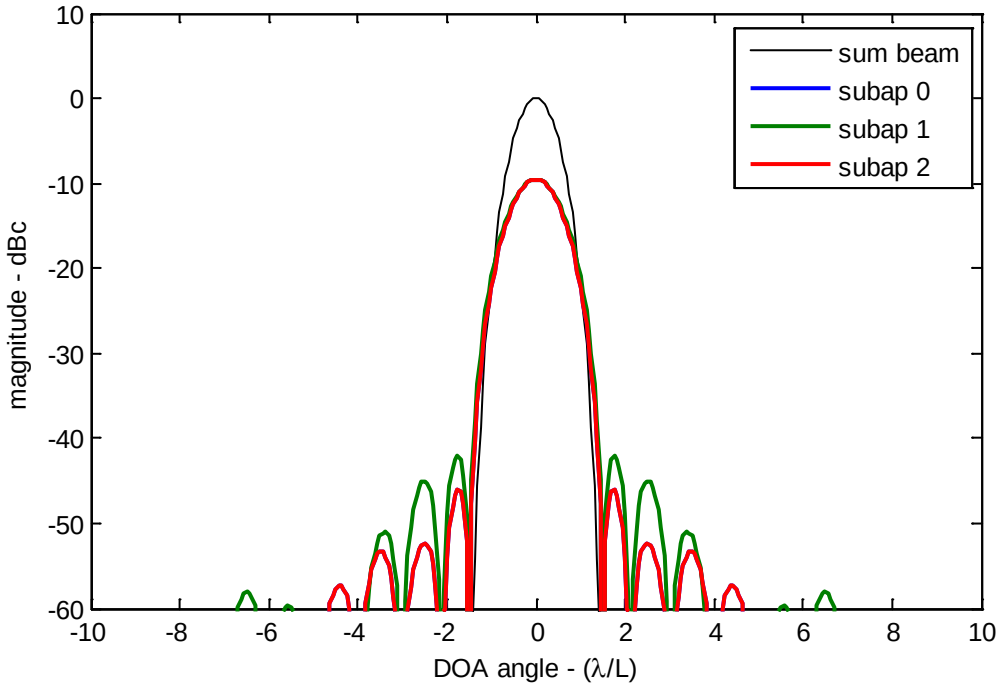

Figure 17. Two-way beam patterns for overall aperture and subapertures.

3.2.2 Four Subapertures

We illustrate with an example that divides the aperture into 4 equal-gain subapertures. Relevant measures are given in Table 5. Figure 18 plots the subapertures and their phase centers. Figure 19 plots the one-way patterns. Figure 20 illustrates the two-way pattern, with the transmitted signal using the sum pattern.

Table 5. Subaperture characteristics for 4 subapertures using -30 dB Taylor window, $\bar{n} = 5$.

Subaperture	*Physical Center (m)*	*Phase Center (m)*	*Width (m)*	*Gain (dBc)*
0	–0.3354	–0.2994	0.3291	–12.0412
1	–0.0854	–0.0828	0.1709	–12.0412
2	0.0854	0.0828	0.1709	–12.0412
3	0.3354	0.2994	0.3291	–12.0412

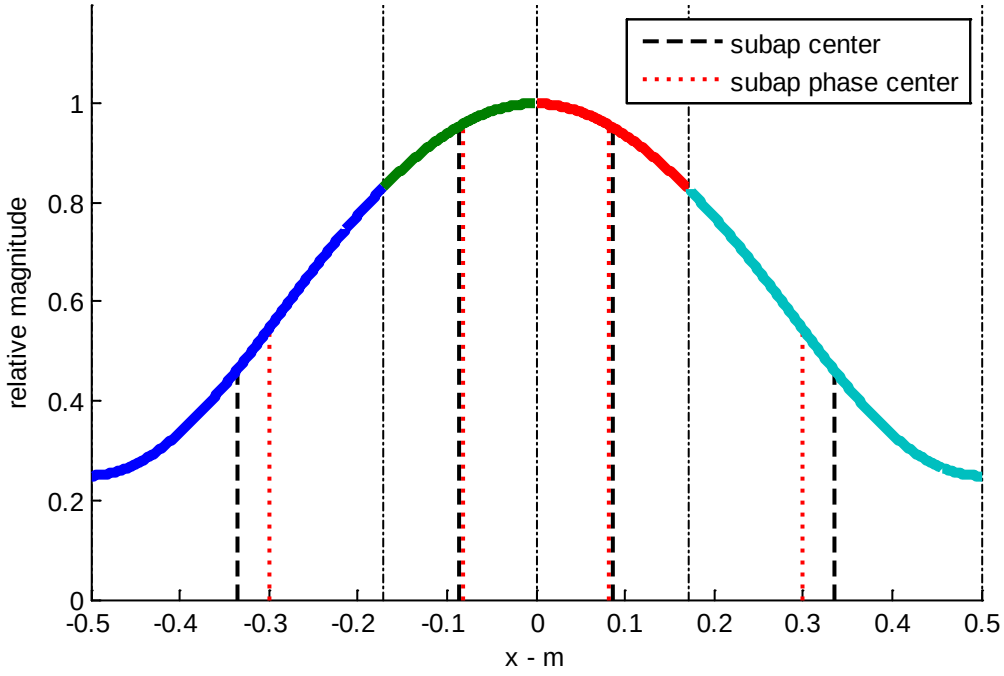

Figure 18. Subaperture definitions and parameters. Overall aperture weighting is –30 dB Taylor window with nbar=5.

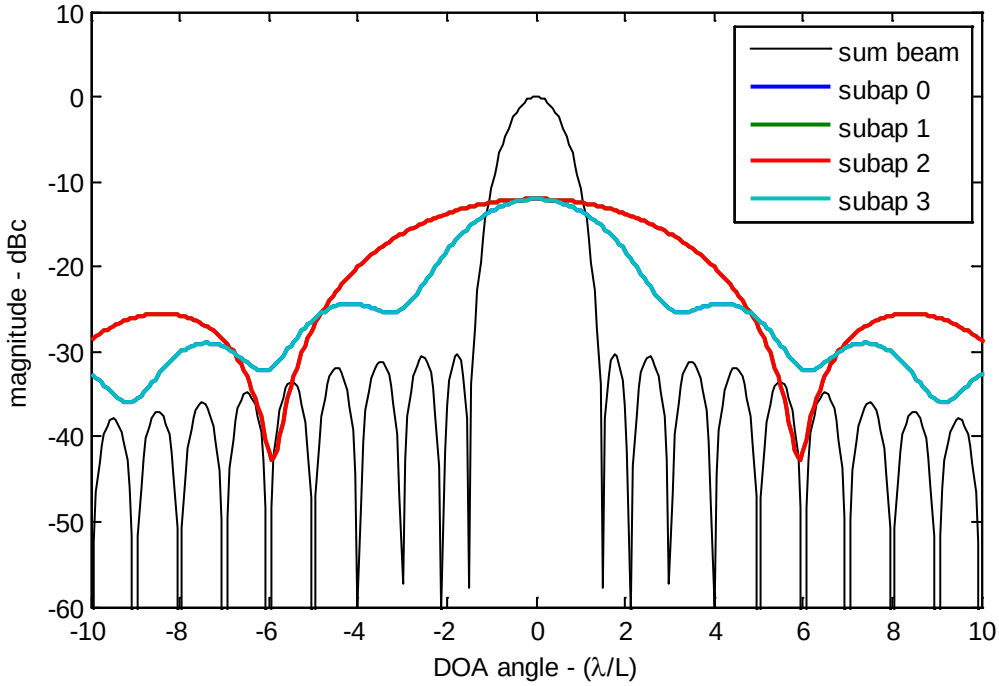

Figure 19. One-way beam patterns for overall aperture and subapertures.

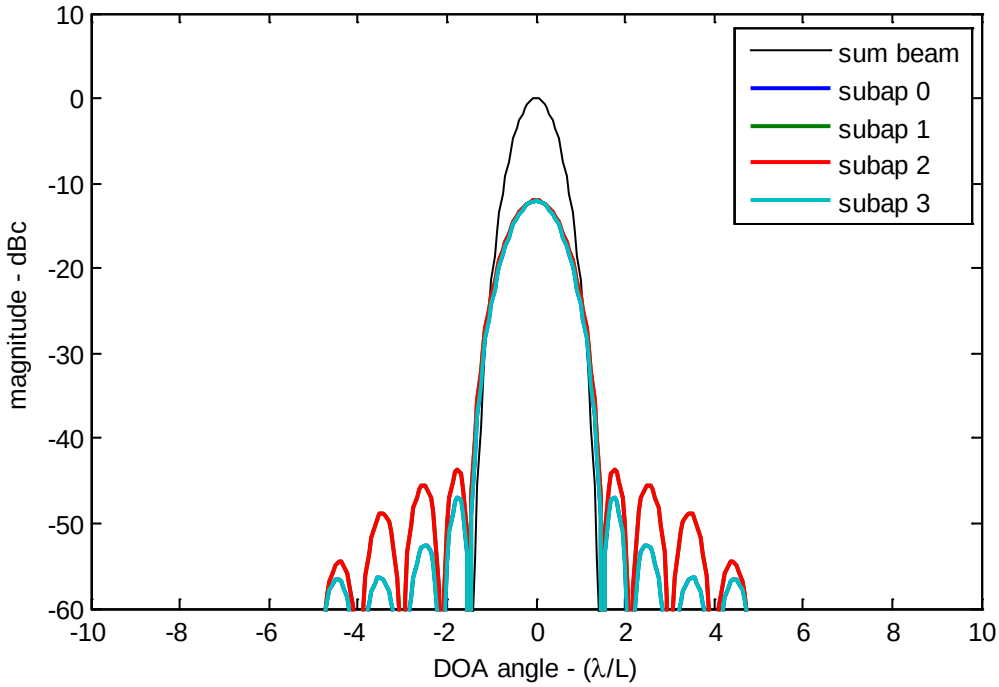

Figure 20. Two-way beam patterns for overall aperture and subapertures.

3.2.3 Five Subapertures

We illustrate with an example that divides the aperture into 5 equal-gain subapertures. Relevant measures are given in Table 6. Figure 21 plots the subapertures and their phase centers. Figure 22 plots the one-way patterns. Figure 23 illustrates the two-way pattern, with the transmitted signal using the sum pattern.

Table 6. Subaperture characteristics for 5 subapertures using -30 dB Taylor window, $\bar{n} = 5$.

Subaperture	*Physical Center (m)*	*Phase Center (m)*	*Width (m)*	*Gain (dBc)*
0	–0.3558	–0.3265	0.2885	–13.9794
1	–0.1382	–0.1351	0.1466	–13.9794
2	0	0	0.1298	–13.9794
3	0.1382	0.1351	0.1466	–13.9794
4	0.3558	0.3265	0.2885	–13.9794

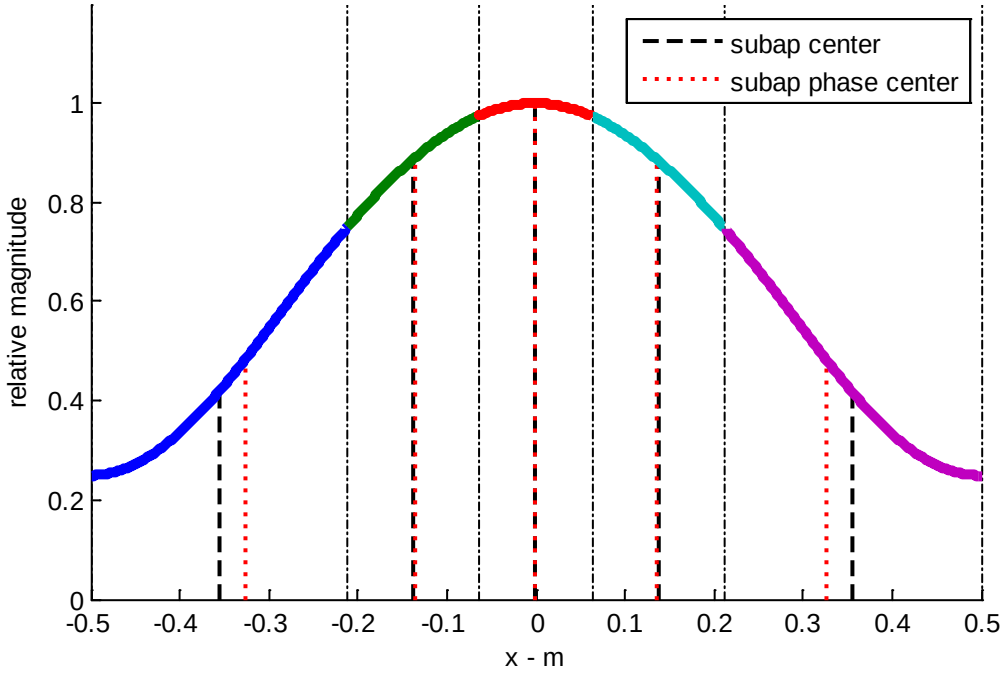

Figure 21. Subaperture definitions and parameters. Overall aperture weighting is –30 dB Taylor window with nbar=5.

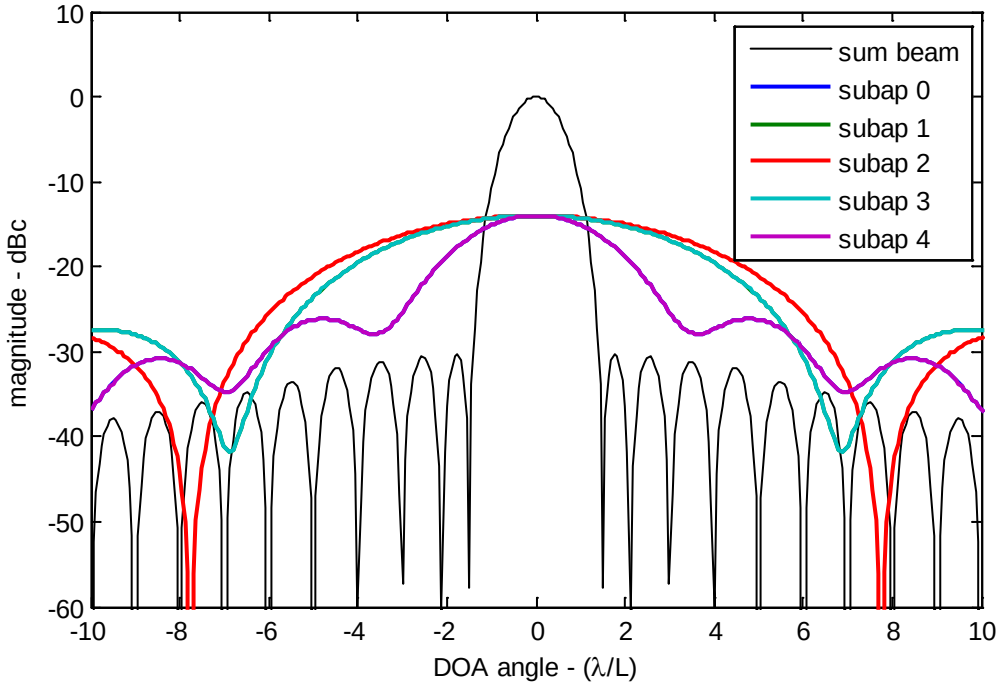

Figure 22. One-way beam patterns for overall aperture and subapertures.

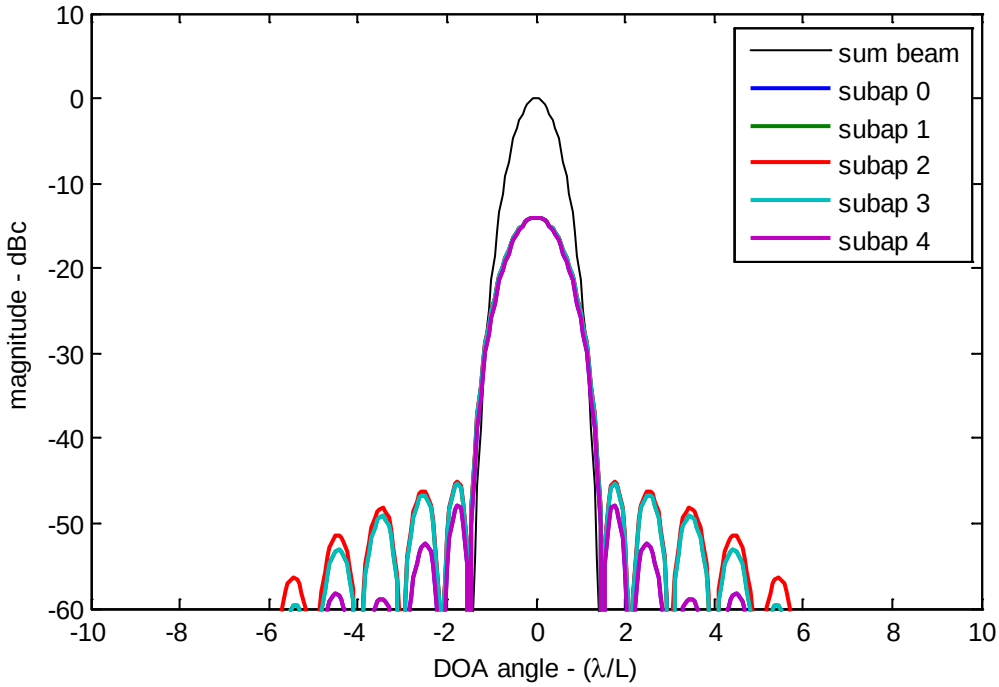

Figure 23. Two-way beam patterns for overall aperture and subapertures.

3.3 Comments

We offer the following comments.

- The width of the mainlobe responses from the individual subaperture beams will always be wider than the width of the mainlobe response of the sum beam.
- For a tapered sum beam with segmented subapertures, uniform-width subapertures will have different maximum gains.
- For a tapered sum beam with segmented subapertures, uniform-maximum-gain subapertures will have different physical widths.
- Tapering the sum beam will draw the phase centers of the individual subapertures inwards, towards the center of the overall aperture.
- Subaperture pattern sidelobes are largely a function of the hard edges at the subaperture boundaries.
- Uniform-maximum-gain subapertures will have the phase centers of their individual subapertures moved inwards somewhat from those of uniform-width subapertures, towards the center of the overall aperture.
- Subapertures with indices i and $I-1-i$ are mirror images of each other, and will each have the same shapes of their beam patterns; same in magnitude but not necessarily in phase. This follows from the Fourier property that the transform of a real function will have symmetry in the magnitude of its spectrum. This is why some subapertures are not visible in some of the previous plots; they are basically covered up by other subapertures' responses.
- Uniform-width subapertures are not guaranteed to yield uniformly-spaced phase centers, especially when $I > 3$. The amount of phase center shift will depend on the local subaperture weighting function.

4 Tapered and Overlapped Subapertures

We now loosen the constraints of the earlier section and allow subapertures to overlap. The purpose is to allow tapering of the subapertures to facilitate subaperture beam sidelobe reduction. Sidelobe control in subaperture architectures are discussed in an earlier report by Doerry.[6] Accordingly we define

$w_i(x)$ = the taper function of the i^{th} subaperture. (32)

We will assume that the subaperture tapers $w_i(x)$ are each nonzero but still real over the interval $[-0.5, 0.5]$, but unlike the overall aperture illumination $w_{ap}(x)$, the subaperture tapers need not be even.

We stipulate, however, that the sum of all the subaperture tapers (suitably shifted) equals the overall aperture taper function, that is

$$w_{ap}\left(\frac{x}{L_{ap}}\right) = \sum_{i=0}^{I-1} w_i\left(\frac{x - x_{1,i}}{L_i}\right). \tag{33}$$

The far-field patterns of the individual subapertures are now calculated as

$$G_i(\theta) = \int_{-\infty}^{\infty} w_i\left(\frac{x - x_i}{L_i}\right) e^{-j\frac{2\pi \sin\theta}{\lambda}x}\, dx. \tag{34}$$

For all subsequent examples, unless otherwise indicated, we shall assume an overall aperture weighting defined by a Taylor window with −30 dB sidelobes and $\bar{n} = 5$. Furthermore, we shall assume

L_{ap} = 1 m, and
λ = 0.02 m. (35)

Subaperture phase centers are calculated using numerical integration.

Figure 24 essentially duplicates the example of Section 3.2.1, with three constant-gain subapertures, albeit with a more expanded view of the far-field beam patterns.

Figure 25 takes the tapers of Figure 24 and feathers the transition (boundary) regions between the subapertures. Each feathering is over an interval of 1/6 of the overall aperture length.

We note that feathering the subapertures will affect phase center locations somewhat.

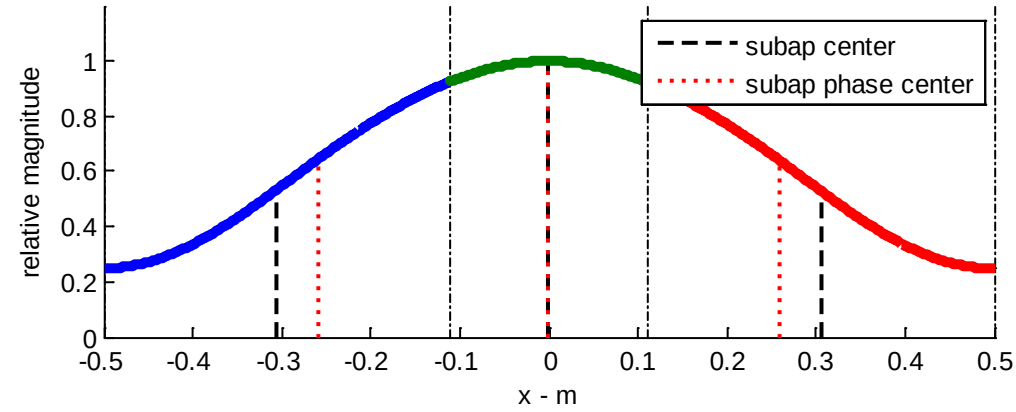

(a)

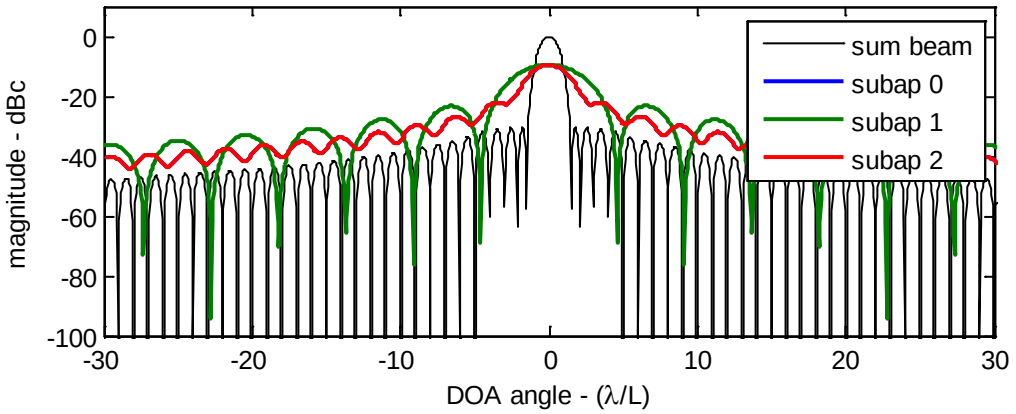

(b)

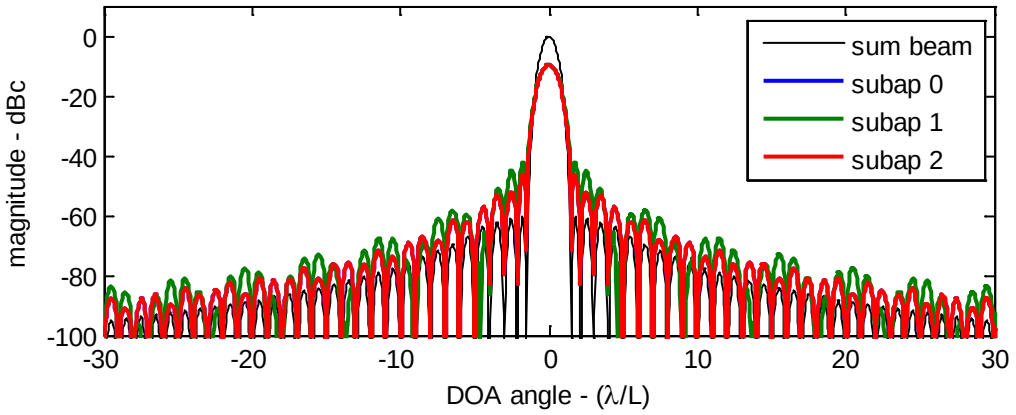

(c)

Figure 24. (a) subaperture illumination function, (b) one-way antenna far-field patterns, (c) two-way far-field patterns. Overall aperture weighting is –30 dB Taylor window with nbar=5.

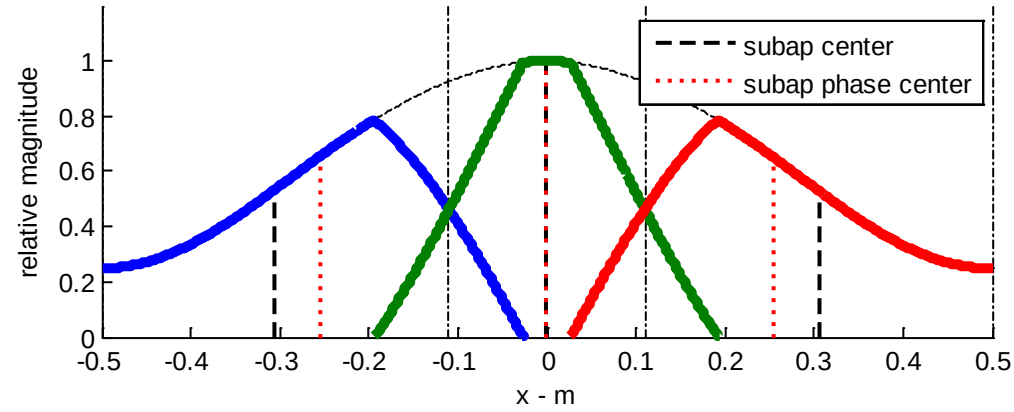

(a)

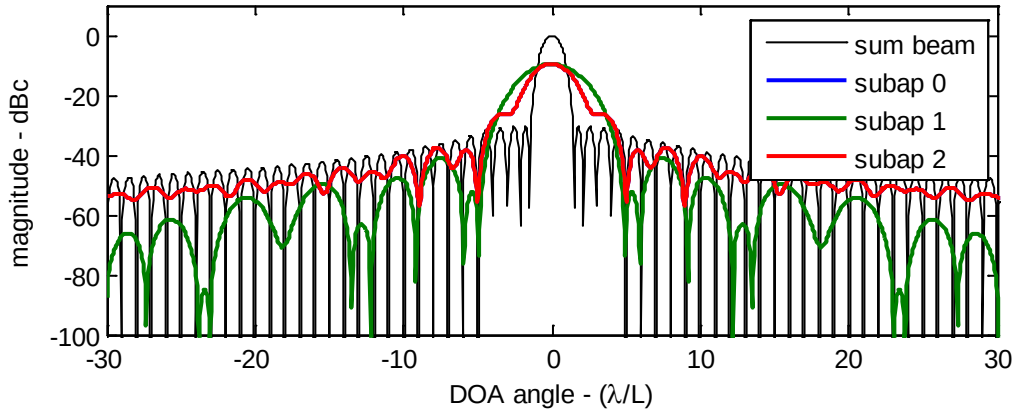

(b)

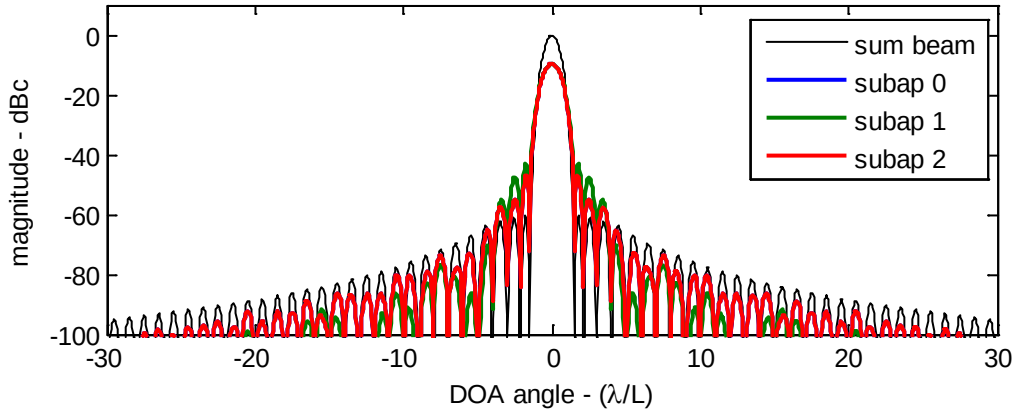

(c)

Figure 25. (a) subaperture illumination function, (b) one-way antenna far-field patterns, (c) two-way far-field patterns. Overall aperture weighting is –30 dB Taylor window with nbar=5.

Comments

We offer the following comments.

- There are three principal regions of interesting behavior, which we illustrate in Figure 26. These are
  1. Within the mainlobe of the sum beam,
  2. Outside the mainlobe of the sum beam, but inside the mainlobe of the individual subaperture beams, and
  3. In the sidelobe region of the individual subaperture beams.

- As one might expect, any additional tapering of the individual subapertures will mainly affect the sidelobes of the subaperture beam patterns (region #3), and not the nature of the two-way response within the mainlobe of the subaperture beams (regions #1 and #2).
- Two-way beam pattern response, including sum pattern sidelobes, within the subaperture mainlobes (regions #1 and #2) will not be affected by additional subaperture tapering.
- Reducing two-way pattern sidelobes within the subaperture mainlobe regions (region #2) can only be accomplished by reducing the sidelobes of the sum pattern response. Figure 27 illustrates the previous examples but with a –50 dB Taylor ($\bar{n} = 7$) weighting function for the overall aperture.
- The question of "How far down do sidelobes need to be?" is a system design question that depends on the allowable likelihood of confusing energy or false targets.[7]

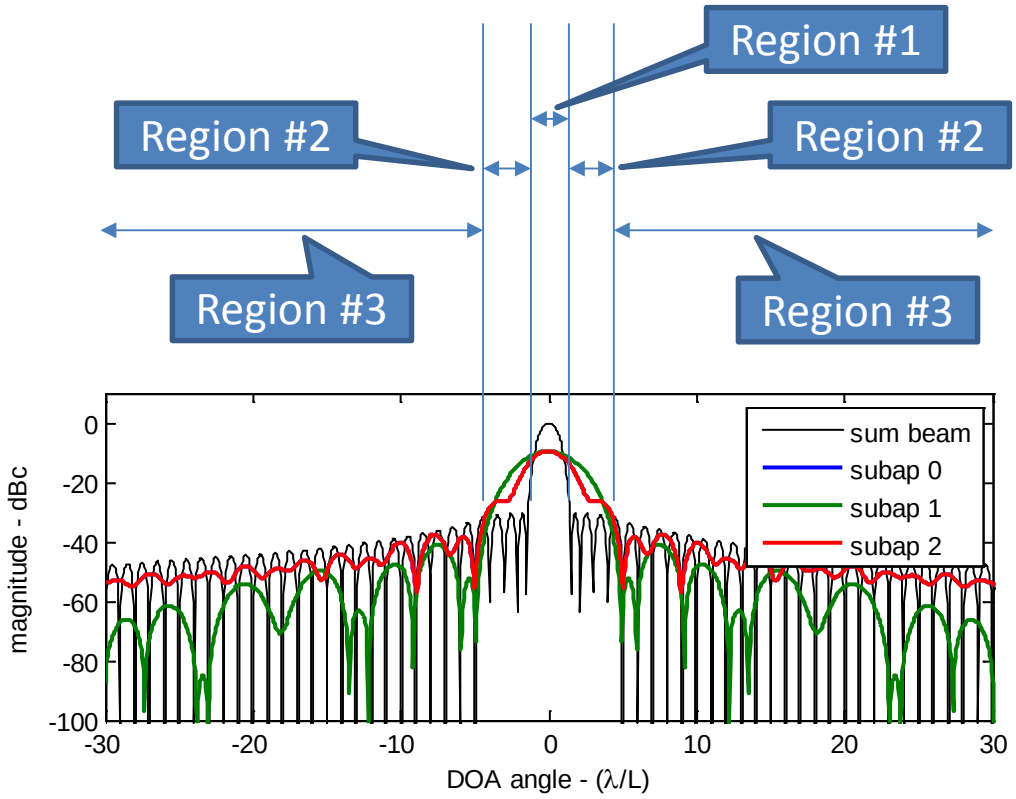

Figure 26. Major regions of interest for sidelobe responses. The plot is the same as Figure 25 (c).

Region 1 - Within the mainlobe of the sum beam,
Region 2 - Outside the mainlobe of the sum beam, but inside the mainlobe of the individual subaperture beams, and
Region 3 - In the sidelobe region of the individual subaperture beams.

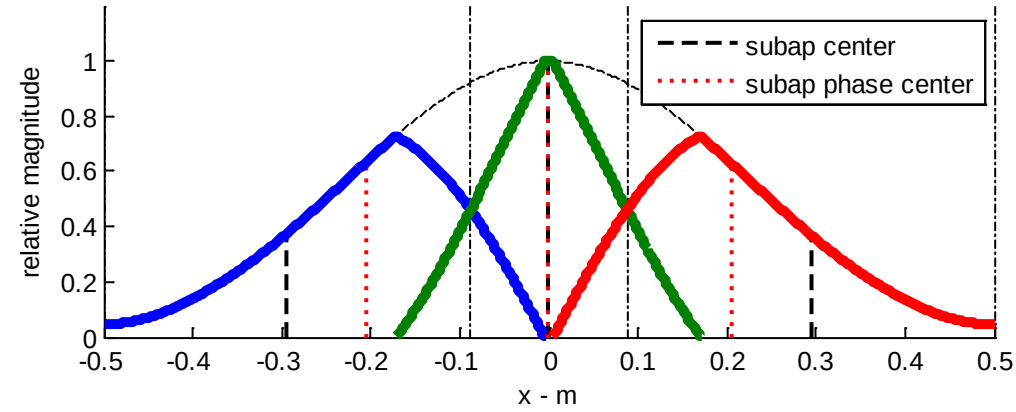

(a)

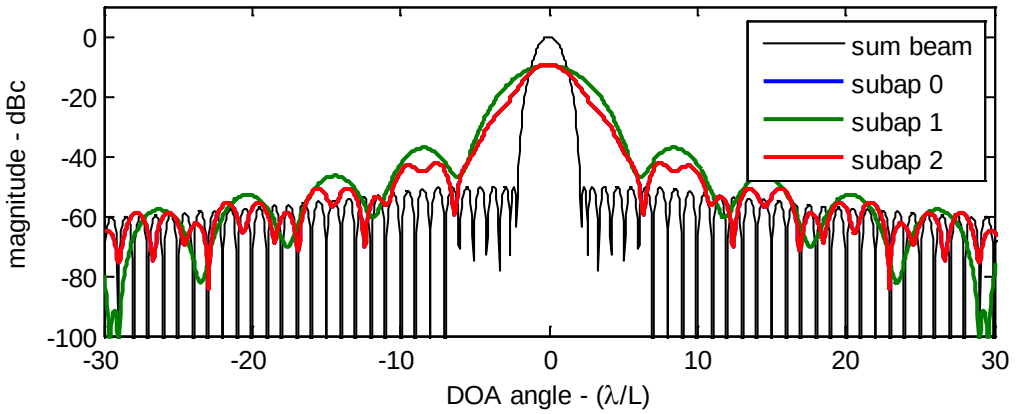

(b)

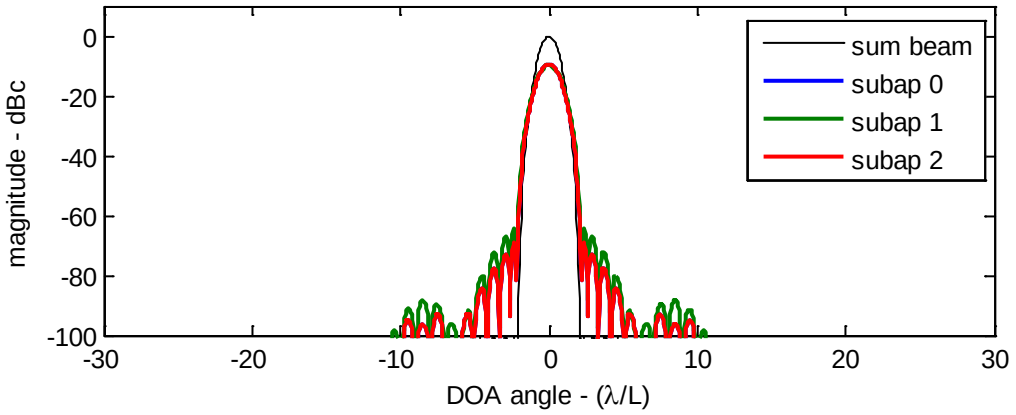

(c)

Figure 27. (a) subaperture illumination function, (b) one-way antenna far-field patterns, (c) two-way far-field patterns. Overall aperture weighting is –50 dB Taylor window with nbar=5.

5 Brief Comments on Performance

Recapping, subapertures in antenna arrays are used to estimate Direction-Of-Arrival (DOA). The subaperture weighting functions affect both the subarray gain and the relative position of phase centers. In DOA estimation, the performance is a function of the Signal-to-Noise Ratio (SNR) and the (projected) separation distance between phase centers, B. In fact the angle estimation noise depends on these as

$$\sigma_\theta \propto \frac{1}{B\sqrt{snr}} \tag{36}$$

The SNR, is in turn a function of the product of the transmit and receive antenna gains (plus any additional processing gain between subarrays for the DOA estimation). As we have just seen in the previous analysis, the subaperture weightings affect both the gains and the phase center separations. Therefore, the radar designer needs to account for these in performing the trade-off between different subaperture weightings.

“There's a way to do it better - find it.”
-- Thomas A. Edison

6 Conclusions

We summarize herein the following key points.

- Uneven subaperture tapering will shift the phase center away from the center of the subaperture, and generally in the direction with greater weighting.

- Subaperture phase center spacing is not guaranteed to be even, even with equal-width subapertures.

- Subaperture gain will not necessarily be identical for all subapertures, although subapertures can be defined to specifically make them so, albeit with other consequences.

“Opportunity is missed by most people because it is dressed in overalls and looks like work.”
-- Thomas A. Edison

References

[1] *IEEE Standard Radar Definitions*, IEEE Std 686™-2008, Sponsored by the Radar Systems Panel, IEEE Aerospace and Electronic Systems Society, 21 May 2008.

[2] Armin W. Doerry, "Just Where Exactly is the Radar? (a.k.a. The Radar Antenna Phase Center)," Sandia National Laboratories Report SAND2013-10635, Unlimited Release, December 2013.

[3] Armin W. Doerry, Douglas L. Bickel, "GMTI Direction of Arrival Measurements from Multiple Phase Centers," Sandia Report SAND2015-2310, Unlimited Release, March 2015.

[4] Armin W. Doerry, Douglas L. Bickel, "Limits to Clutter Cancellation in Multi-Aperture GMTI Data," Sandia Report SAND2015-2311, Unlimited Release, March 2015.

[5] Armin W. Doerry, Douglas L. Bickel, "Single-Axis Three-Beam Amplitude Monopulse Antenna – Signal Processing Issues," Sandia Report SAND2015-4113, Unlimited Release, May 2015.

[6] Armin W. Doerry, "Window Taper Functions for Subaperture Processing," Sandia Report SAND2013-10619, Unlimited Release, December 2013.

[7] A. W. Doerry, D. L. Bickel, A. M. Raynal, "Some comments on performance requirements for DMTI radar," SPIE 2014 Defense & Security Symposium, Radar Sensor Technology XVIII, Vol. 9077, Baltimore MD, 5–9 May 2014.

Distribution

Unlimited Release

1	MS 0519	J. A. Ruffner	5349	
1	MS 0519	A. W. Doerry	5349	
1	MS 0519	L. Klein	5349	
1	MS 0519	D. L. Bickel	5344	
1	MS 0532	S. P. Castillo	5340	
1	MS 0899	Technical Library	9536	(electronic copy)

Sandia National Laboratories